J. Fluid Mech. (1994), *vol.* 258, *pp.* 115–129

Crest instabilities of gravity waves. Part 1. The almost-highest wave

By MICHAEL S. LONGUET-HIGGINS[1] AND R. P. CLEAVER[2]

[1] Institute for Nonlinear Science, University of California, San Diego, La Jolla, CA 92093-0402, USA

[2] Gas Research Centre, British Gas, Ashby Road, Loughborough, LE11 3QU, UK

(Received 16 April 1993 and in revised form 17 June 1993)

It is shown theoretically that the crest of a steep, irrotational gravity wave, considered in isolation, is unstable. There exists just one basic mode of instability, whose exponential rate of growth β equals $0.123(g/R)^{\frac{1}{2}}$, where g denotes gravity and R is the radius of curvature at the undisturbed crest. A volume of water near the crest is shifted towards the forward face of the wave; the 'toe' of the instability is at a horizontal distance $0.45R$ ahead of the crest. The instability may represent the initial stage of a spilling breaker. On small scales, the 'toe' may be a source of parasitic capillary waves.

1. Introduction

Despite much interest during the last twenty years, the problem of how and why gravity waves break in deep water has remained incompletely solved; for recent reviews see Longuet-Higgins (1988) and Banner & Peregrine (1993).

As pointed out previously (Longuet-Higgins 1981), a breaking wave does not necessarily pass through the limiting configuration for steady, steep irrotational waves first calculated by Michell (1893), with a sharp angle of 120° at the crest (the 'Stokes corner-flow'). The actual flow being unsteady, this limiting configuration is by-passed, by a less or greater margin. Thus from observation it is found that the mean ratio H/L of height H to wavelength L in a breaking wave is usually less than the value 0.141 for limiting waves. The latter would correspond to a 'steepness' parameter $ak = \pi H/L = 0.443$. For breakers resulting from the fastest-growing Benjamin–Feir instability it is found that $ak \approx 0.38$ (see Longuet-Higgins & Cokelet 1978, figure 22(*c*)). In a typical sea-state, ak may lie between 0.05 and 0.20 (see Holthuijsen & Herbers 1986).

The Benjamin–Feir instability also does not account for the marked horizontal asymmetry of steep waves prior to breaking (Kjeldsen & Myrhaug 1980; Bonmarin 1990), although Tulin & Li (1991) have shown that this type of instability does produce an increased supply of energy to the forward face of the wave.

The general approach of regarding the initial stages of wave breaking as being due to an instability of a steady flow is attractive, however. In the present paper we consider first the instability of a single, steep wave crest, as described by the theory of the 'almost-highest' wave (Longuet-Higgins & Fox 1977, 1978). This theory describes the flow near the crest of any steady, irrotational wave having slightly less than the maximum height. The curvature of the surface profile is everywhere finite. In the 'inner flow' the surface slope tends to 120° in each direction. We here consider time-dependent perturbations of this flow. If the crest is perturbed by the addition of extra energy, how does the deformation develop? What are the normal modes of

perturbation? If any of the modes are unstable, which mode has the fastest rate of growth? How does this compare with observation?

The method of analysis is similar to that developed earlier for periodic progressive waves in deep water (Longuet-Higgins 1978*a*, *b*). Here, however, it is applied to an isolated wave crest; the lengthscales in the basic flow and its perturbations are assumed small compared to a wavelength L. As will be shown, there do indeed exist both time-periodic normal-mode perturbations and an exponentially growing normal mode, with a characteristic rate of growth.

A further reason for interest in this problem may be mentioned. It is known that a steep, fairly short gravity wave, with wavelength of order 10 cm, can develop parasitic capillary waves on its forward face, leading sometimes to a 'capillary bore' (see Longuet-Higgins 1992). The question arises: how is such a bore initiated? Is it due to capillarity combined with the sharp curvature at the wave crest, as is currently believed, or does it arise from an instability of the gravity wave crest?

The work will be presented in two papers. In the present paper, §§2–4, we first describe an improved calculation of the inner flow, making use of some new relations corresponding to the quadratic relations between Stokes's coefficients in periodic waves. In §§5 and 6 we proceed to give a method for calculating the perturbations of the inner flow, and the corresponding results. These are discussed in Section 7.

In a second paper (Longuet-Higgins, Cleaver & Fox 1994) we will describe the corresponding results when the lowest-order correction to the outer flow is included in the calculations.

2. The almost-highest wave: definitions

Consider a steady irrotational wave propagating to the left with speed c as in figure 1. In a frame of reference moving with the phase speed the flow appears steady, and we may take rectangular coordinates (x, y) with the x-axis horizontal, the y-axis upwards and the origin 0 vertically above a wave crest, at such a distance that Bernoulli's equation can be written,

$$p + y + \tfrac{1}{2}q^2 = 0, \tag{2.1}$$

where p is the pressure, and q the particle speed. We have chosen the units of mass and time so that the density ρ and the acceleration due to gravity g are both unity. On the free surface $p = 0$ we have then

$$2y + q^2 = 0. \tag{2.2}$$

If ϕ and ψ denote the velocity potential and the stream function respectively, then on the free surface we may take $\psi = 0$. Further writing $z = \mathrm{i}(x + \mathrm{i}y)$ and $\chi = \phi + \mathrm{i}\psi$ we have

$$2y = -(z + z^*), \quad q^2 = \chi_z \chi_z^* = (z_\chi z_\chi^*)^{-1} \tag{2.3}$$

so that (2.2) becomes simply

$$(z + z^*) z_\chi z_\chi^* = 1. \tag{2.4}$$

For very steep waves the dimensionless parameter

$$\epsilon = q_0/\sqrt{2c} \tag{2.5}$$

becomes small, q_0 being the particle speed at the crest ($\chi = 0$). It was shown by Longuet-Higgins & Fox (1977, 1978) that as $\epsilon \to 0$ the flow near the wave crest tends asymptotically to a certain 'inner solution', described in Longuet-Higgins & Fox (1977, referred to herein as LHF1). As unit of length we may choose the vertical distance of the wave crest from the origin $x = 0$; see figure 1. Then at the crest ($\chi = 0$) we have

$$y = -1, \quad q = q_0 = \sqrt{2}, \tag{2.6}$$

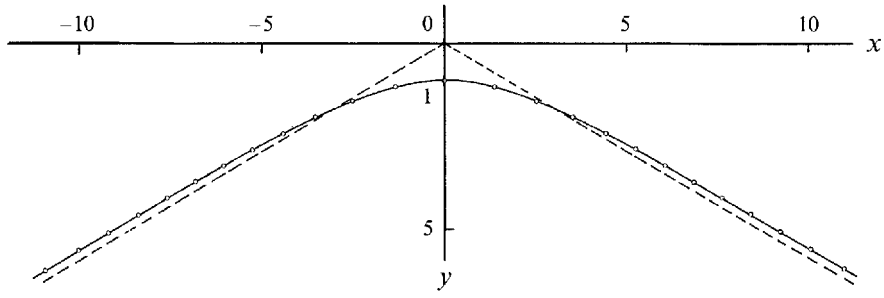

FIGURE 1. Profile of the almost-highest wave, showing coordinates and the 30° asymptotes (from LHF1).

by (2.2). For large values of z the inner flow tends to Stokes's 120° corner flow,

$$z \sim (\tfrac{3}{2}\mathrm{i}\chi)^{\frac{2}{3}} \quad \text{as} \quad z \to \infty. \tag{2.7}$$

To calculate the complete inner flow LHF1 make the transformation

$$\omega = \frac{\beta - \mathrm{i}\chi}{\beta + \mathrm{i}\chi}, \quad \mathrm{i}\chi = \beta \frac{1-\omega}{1+\omega}, \tag{2.8}$$

where β is a positive constant, and then suppose that inside the circle $|\omega| = 1$ (which corresponds to the fluid domain $\psi < 0$) the solution can be expressed in the form

$$z = (\delta + \mathrm{i}\chi)^{\frac{2}{3}} B(\omega), \tag{2.9}$$

where δ is a positive constant and

$$B(\omega) = B_0 + B_1 \omega + B_2 \omega^2 + \ldots \tag{2.10}$$

is a power series in ω with real coefficients B_n. It is convenient to take $\delta = \beta$. To ensure that the free surface passes through the wave crest, where $\chi = 0$, $\omega = 1$, we must specify that

$$B(1) = B_0 + B_1 + B_2 + \ldots = \delta^{-\frac{2}{3}}. \tag{2.11}$$

Since the coefficients B_n are all real, the flow will be symmetric about the line $x = 0$.

Now to satisfy the free-surface condition (2.4), we have from (2.9)

$$z_\chi = \mathrm{i}(\delta + \mathrm{i}\chi)^{-\frac{1}{3}} H(\omega), \tag{2.12}$$

where

$$H(\omega) = \tfrac{2}{3} B(\omega) - (1+\omega) B'(\omega) \tag{2.13}$$

and a prime denotes $\mathrm{d}/\mathrm{d}\omega$. The boundary condition (2.4) then becomes

$$[\omega^{-\frac{1}{3}} B(\omega) + \omega^{\frac{1}{3}} B(\omega^{-1})]\, H(\omega)\, H(\omega^{-1}) = 1, \tag{2.14}$$

to be satisfied on the circle $|\omega| = 1$ when $\tau = \arg \omega$ lies in the open interval $(-\pi, \pi)$. Since $\omega^{-\frac{1}{3}}$ may be expanded in a Fourier series:

$$\omega^{-\frac{1}{3}} = \sum_{-\infty}^{\infty} K_n \omega^n, \tag{2.15}$$

where

$$K_n = \frac{\sin(n + \frac{1}{3})\pi}{(n + \frac{1}{3})\pi}, \quad n = 0, \pm 1, \pm 2, \ldots, \tag{2.16}$$

we can substitute into the boundary condition (2.14) and by equating coefficients of $\cos n\tau$ obtain an infinite set of *cubic* equations for the coefficients B_n.

In LHF1 this system of equations was solved numerically, together with (2.10), taking $\delta = 10^{\frac{3}{2}}$. On successive truncation of the system at increasing values of n a solution was found which converged satisfactorily. The profile of the free surface is plotted in figure 9 of LHF1.

We shall now show how the system of cubic equations for the coefficients B_n can with advantage be replaced by an equivalent set of quadratic equations. This not only enables the basic inner flow to be calculated with greater accuracy, but it considerably simplifies the analysis of the normal-mode perturbations, which is our present objective.

3. Quadratic equations for the coefficients B_n

The boundary condition (2.14) can be written

$$L(\omega)\,H(\omega)\,H(\omega^{-1}) = 1 \quad \text{on} \quad |\omega| = 1, \tag{3.1}$$

where

$$L(\omega) = \omega^{-\frac{1}{3}}B(\omega) + \omega^{\frac{1}{3}}B(\omega^{-1}) = \sum_{-\infty}^{\infty} L_n\,\omega^n \tag{3.2}$$

and

$$H(\omega) = \tfrac{2}{3}B(\omega) - (1+\omega)\,B'(\omega) = \sum_{0}^{\infty} H_n\,\omega^n, \tag{3.3}$$

say. From (2.15) we have

$$\left.\begin{aligned} L_0 &= (K_0 + K_0\ )\,B_0 + (K_{-1}+K_{-1})\,B_1 + (K_{-2}+K_{-2})\,B_2 + \ldots, \\ L_1 &= (K_1 + K_{-1})\,B_0 + (K_0\ \ + K_{-2})\,B_1 + (K_{-1}+K_{-3})\,B_2 + \ldots, \\ L_2 &= (K_2 + K_{-2})\,B_0 + (K_1\ \ + K_{-3})\,B_1 + (K_0\ \ + K_{-4})\,B_2 + \ldots, \\ &\vdots \end{aligned}\right\} \tag{3.4}$$

and since $L(\omega)$ is real, $L_{-n} = L_n$. The coefficients $L_0, L_1, \ldots$ are linear combinations of the B_n and are real also.

Consider now the product

$$M(\omega) = L(\omega)\,H(\omega) = \sum_{-\infty}^{\infty} M_n\,\omega^n, \tag{3.5}$$

say. The boundary condition (3.1) can be written

$$N(\omega) \equiv M(\omega)\,H(\omega^{-1}) = 1 \quad \text{on} \quad |\omega| = 1. \tag{3.6}$$

The coefficient N_n of ω^n in $N(\omega)$ is a cubic function of the B_n, formally identical to N_{-n}, since $N(\omega)$ was constructed as a real function of ω (N is symmetric with regard to τ). So in order to satisfy (3.1) we have only to equate coefficients of the *non-negative* powers of ω in (3.6). This yields

$$\left.\begin{aligned} M_0H_0 + M_1H_1 + M_2H_2 + \ldots + M_nH_n\ \ + \ldots &= 1, \\ M_1H_0 + M_2H_1 + \ldots + M_nH_{n-1} + \ldots &= 0, \\ M_2H_0 + \ldots + M_nH_{n-2} + \ldots &= 0, \\ &\vdots \\ M_nH_0 + \ldots &= 0. \end{aligned}\right\} \tag{3.7}$$

If we truncate the system by assuming $M_n = 0$ when $n > m$, say, we get a set of m linear equations for $M_0, M_{-1}, \ldots, M_{-M}$ with matrix

$$\begin{pmatrix} H_0 & H_1 & H_2 & \ldots & H_m \\ 0 & H_0 & H_1 & \ldots & H_{m-1} \\ 0 & 0 & H_0 & \ldots & H_{m-2} \\ 0 & 0 & 0 & \ldots & H_0 \end{pmatrix}, \tag{3.8}$$

which has non-vanishing determinant H_0^m. Thus (3.7) has the unique solution

$$M_0 = 1/H_0, \quad M_1 = M_2 = \ldots = M_m = 0. \tag{3.9}$$

Allowing m to go to infinity we obtain an infinite set of equations which is quadratic in the B_n. In fact from (3.5) we obtain

$$\left.\begin{aligned} L_0 H_0 + L_{-1} H_1 + L_{-2} H_2 + \ldots &= 1/H_0, \\ L_1 H_0 + L_0 \ H_1 + L_{-1} H_2 + \ldots &= 0, \\ L_2 H_0 + L_1 H_1 \ + L_0 \ H_2 + \ldots &= 0. \end{aligned}\right\} \tag{3.10}$$

Conversely it may be shown that any set of coefficients B_n satisfying the (mainly) quadratic system (3.10) also satisfies the cubic system (3.7) and hence the boundary condition.

We remark that the coefficients $M_{-1}, M_{-2}, \ldots$ do not in general vanish. They are the coefficients in the expansion of $1/H(\omega)$ in a series of negative powers of ω.

The relations (3.10) are closely analogous to the quadratic relations found by Longuet-Higgins (1978*a*) between the coefficients in Stokes's expansion for periodic waves in deep water.

4. Recalculation of the inner solution

Setting $B_n = 0$ for $n > N$, say, the system of equations

$$\left.\begin{aligned} H_0 M_0 &= 1, \\ M_n &= 0, \quad n = 1, 2, \ldots (N-1), \\ \sum_0^m B_n &= \delta^{-\frac{2}{3}}, \quad \delta = 10^{\frac{3}{2}} \end{aligned}\right\} \tag{4.1}$$

were solved for $B_0, B_1, \ldots, B_N$ using Newton's method of approximation with a standard subroutine for matrix inversion. The set (4.1) may be solved much more speedily than the set obtained from (3.7). For $N = 90$, say, the values of $B_0, \ldots, B_{20}$ agreed with the values given in LHF1, table 2, to all the quoted decimal places. The nature of the convergence of the B_n is shown in figure 2, where $\ln|B_N|$ is plotted against $\ln n$ for $n = 1, \ldots, 90$. When $1 \leqslant n \leqslant 6$ the coefficients decrease roughly like $n^{-2.5}$. When $14 < n < 60$ the even coefficients decrease like $n^{-4.4}$, as indicated. The change in power law comes at about $n = 10$. Until $n = 29$ (the same order as δ) all the coefficients after B_0 are negative. When $n \geqslant 30$ they alternate in sign, with $B_n \gtrless 0$ as n is even or odd. After $n = 30$ the differences between odd and even values of $|B_n|$ diminish, and by $n = 60$ they are very small. Beyond $n = 60$ the decay is more rapid than a power law, and is possibly exponential.

The series for $B(\omega)$ and $H(\omega)$ were checked by inserting them in the boundary condition (2.4). When $N = 90$, for example, the difference between the left- and right-hand sides was found to be less than 5×10^{-5} for all $|z| < 68.5$ (the second crossing of the asymptote). If use was made of Padé approximants, based on either the odd or the even coefficients, the residuals were reduced to less than 10^{-10}. The agreement with the asymptotic expressions for the outer part of the flow (see LHF1, §4) was even closer than that shown in figure 8 of LHF1.

We proceed now to define and calculate the normal-mode perturbations to this flow.

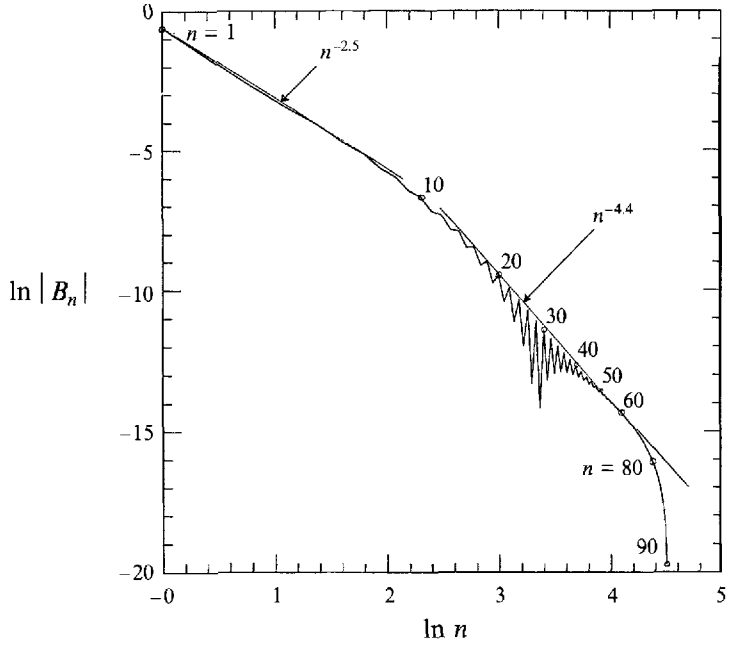

FIGURE 2. Plot of $\ln|B_n|$ *vs.* $\ln n$ when $n = 1, \ldots, 90$, showing the asymptotic behaviour of the coefficients.

5. Small perturbations: method of approach

To derive the equations governing small perturbations of the inner flow we use the general method introduced by Longuet-Higgins (1978*b*) which was applied there to the calculation of the normal-mode perturbations of a periodic Stokes wave. Thus if we take as independent variables the velocity potential ϕ and the stream function ψ in the perturbed motion, together with the time t, the free surface may be specified by

$$\psi = F(\phi, t) \tag{5.1}$$

and the two boundary conditions (kinematic and dynamic) when transformed to the new variables become

$$(y_\phi y_t + y_\psi x_t) = (y_\phi^2 + y_\psi^2)\, y = \tfrac{1}{2} \tag{5.2}$$

and

$$(y_\psi y_t - y_\phi x_t) = (y_\phi^2 + y_\psi^2) F_t + [1 - (y_\phi y_t + y_\psi x_t)] F_\phi \tag{5.3}$$

respectively, to be satisfied when $\psi = F$. We now write

$$x = X(\phi, \psi) + \xi(\phi, \psi, t), \quad y = Y(\phi, \psi) + \eta(\phi, \psi, t), \tag{5.4}$$

where X and Y represent the unperturbed flow and ξ and η are small perturbations of the same order as F. On substituting these expressions into (5.2) and (5.3), expanding in a Taylor series about $\psi = 0$ the lowest-order terms give

$$2Y(Y_\phi^2 + Y_\psi^2) = -1 \tag{5.5}$$

as for the steady flow, and the terms of order F give

$$Y_\psi \xi_t + Y_\phi \eta_t = (Y_\phi^2 + Y_\psi^2)\eta + 2Y(Y_\phi \eta_\phi + Y_\psi \eta_\psi) + [Y(Y_\phi^2 + Y_\psi^2)]_\psi F \tag{5.6}$$

and

$$Y_\phi \xi_t - Y_\psi \eta_t = F_\phi + (Y_\phi^2 + Y_\psi^2) F_t, \tag{5.7}$$

both equations to be satisfied on $\psi = 0$.

It is convenient to write

$$\zeta = -\eta + \mathrm{i}\xi, \quad Z = -Y + \mathrm{i}X. \tag{5.8}$$

Then on subtracting i times (5.7) from (5.6) we have

$$\begin{aligned} Z_\chi^*(\zeta_t + \mathrm{i} Z_\chi F_t) = &-\tfrac{1}{2} Z_\chi Z_\chi^* (\zeta + \zeta^*) - \tfrac{1}{2}(Z + Z^*)(Z_\chi^* \zeta_\chi + Z_\chi \zeta_\chi^*) \\ &+ \tfrac{1}{2}\mathrm{i}[(Z + Z^*)(Z_\chi Z_{\chi\chi}^* - Z_\chi^* Z_{\chi\chi}) + (Z_\chi^* - Z_\chi) Z_\chi Z_\chi^*] F \\ &- \mathrm{i} F_\phi \end{aligned} \tag{5.9}$$

to be satisfied on $\mathrm{Im}(\chi) = 0$.

We now assume that the perturbation ζ may be expanded in a series of positive powers of ω and that F may be expanded in a Fourier series on the unit circle: that is

$$\zeta = \sum_{n=0}^{\infty} (b_n + \mathrm{i} a_n)\, \omega^n, \qquad F = \sum_{n=0}^{\infty} (c_n \cos n\tau + d_n \sin n\tau), \tag{5.10}$$

where a_n, b_n, c_n and d_n are time-dependent coefficients. As in Longuet-Higgins (1978*b*), we can always choose the origin of ψ so that $c_0 = 0$.

To expand the boundary condition (5.9) in power series we write, following equation (2.10),

$$\left.\begin{aligned} z &= \Delta^2\ (1+\omega)^{-\frac{2}{3}} B(\omega), \\ z_\chi &= \mathrm{i}\Delta^{-1}(1+\omega)^{\frac{1}{3}} H(\omega), \\ z_{\chi\chi} &= \Delta^{-4}(1+\omega)^{\frac{4}{3}} G(\omega), \end{aligned}\right\} \tag{5.11}$$

where $\Delta = (2\delta)^{\frac{1}{3}}$, $H(\omega)$ is given by (2.13) and

$$G(\omega) = \tfrac{2}{9} B(\omega) - \tfrac{2}{3}(1+\omega) B'(\omega) - (1+\omega)^2 B''(\omega). \tag{5.12}$$

For the perturbation ζ we write

$$\zeta = C(\omega), \qquad \zeta_\chi = -\mathrm{i}\Delta^{-3}(1+\omega) E(\omega), \tag{5.13}$$

where

$$E(\omega) = (1+\omega) C'(\omega). \tag{5.14}$$

Then (5.9) becomes

$$\begin{aligned} -\mathrm{i}\frac{\partial}{\partial t}[P(\omega) C(\omega) - R(\omega) F(\tau)] = \mathrm{Re}\,[Q(\omega) E(\omega) - R(\omega) C(\omega)] \\ + 2\mathrm{i}\left[\left(1 + \cos\tau \frac{\mathrm{d}F}{\mathrm{d}\tau}\right) + S(\omega) F(\tau)\right], \end{aligned} \tag{5.15}$$

where

$$\left.\begin{aligned} P(\omega) &= \Delta^2 (1+\omega^{-1})^{\frac{1}{3}} H(\omega^{-1}), \\ Q(\omega) &= \Delta (1+\omega)^{\frac{2}{3}} [\omega^{-\frac{1}{3}} B(\omega) + \omega^{\frac{1}{3}} B(\omega^{-1})]\, H(\omega^{-1}), \\ R(\omega) &= \Delta (1+\omega)^{\frac{1}{3}} (1+\omega^{-1})^{\frac{1}{3}} H(\omega)\, H(\omega^{-1}), \\ S(\omega) &= \mathrm{Re}\,[(1+\omega)\, \omega^{-\frac{1}{3}} H(\omega)\, H(\omega^{-1})\, H(\omega) \\ &\quad - \{\omega^{-\frac{1}{3}} B(\omega) + \omega^{\frac{1}{3}} B(\omega^{-1})\}\, (1+\omega)\, H(\omega^{-1})\, G(\omega)]. \end{aligned}\right\} \tag{5.16}$$

We may express each of P, Q, R and S as power series in ω:

$$\left.\begin{aligned} P(\omega) &= \sum_{-\infty}^{\infty} P_n \omega^n, \quad Q(\omega) = \sum_{-\infty}^{\infty} Q_n \omega^n, \\ R(\omega) &= \sum_{-\infty}^{\infty} R_n \omega^n, \quad S(\omega) = \sum_{-\infty}^{\infty} S_n \omega^n, \end{aligned}\right\} \tag{5.17}$$

where clearly

$$P_n = 0 \quad \text{when} \quad n > 0. \tag{5.18}$$

From (3.1) it also follows that

$$Q(\omega) = \Delta (1+\omega)^{\frac{2}{3}} / H(\omega) \tag{5.19}$$

and so

$$Q_n = 0 \quad \text{when} \quad n < 0. \tag{5.20}$$

From their original forms in (5.15), R and S are symmetric functions of τ, so

$$R_{-n} = R_n, \quad S_{-n} = S_n \tag{5.21}$$

and we can write

$$R(\tau) = R_0 + 2\sum_1^\infty R_n \cos n\tau, \qquad S(\tau) = S_0 + 2\sum_1^\infty S_n \cos n\tau. \tag{5.22}$$

The two original free-surface conditions are retrieved from the real and imaginary parts of (5.15):

$$\left.\begin{aligned} \frac{\partial}{\partial t}\mathrm{Im}\,[P(\omega)\,C(\omega)] &= \mathrm{Re}\,[Q(\omega)\,E(\omega) - R(\omega)\,C(\omega)] + S(\tau)\,F(\tau), \\ \frac{\partial}{\partial t}\{\mathrm{Re}\,[P(\omega)\,C(\omega)] - R(\tau)\,F(\tau)\} &= -2(1+\cos\tau)\frac{\mathrm{d}F}{\mathrm{d}\tau}. \end{aligned}\right\} \tag{5.23}$$

Equating coefficients of $\cos n\tau$ and $\sin n\tau$ in each of these equations gives four simultaneous equations for the vector

$$\boldsymbol{x} = (a_0, a_1, \ldots;\ b_0, b_1, \ldots;\ c_1, c_2, \ldots;\ d_1, d_2, \ldots); \tag{5.24}$$

see the Appendix. These four equations all have real coefficients. We now seek normal-mode solutions in which $\partial/\partial t \sim \beta$. Thus equations (5.23) yield a matrix equation of the form

$$\beta \boldsymbol{A}\boldsymbol{x} = \boldsymbol{B}\boldsymbol{x}, \tag{5.25}$$

where $\boldsymbol{A}$ and $\boldsymbol{B}$ are matrices of infinite order. Truncating the vector $\boldsymbol{x}$ by setting $B_n = 0$ when $n > N$, say, and letting a_n, b_n, c_n, d_n also vanish when $n > N$, we can choose $(4N+2)$ of the equations (5.25) to determine a sequence of eigenfrequencies σ_j and the corresponding eigenvectors $\boldsymbol{x}_j$. Further details are given in the Appendix.

6. Results

The computations were programmed in FORTRAN (double or quadruple precision), with the aid of a CLAMS library routine SGEEV for extracting the eigenvalues and eigenvectors of a real, non-symmetric square matrix, of order $(2N+1)$ (see the Appendix). The lower eigenvalues, for $N = 30(2)50$ are shown in table 1. They appear to have converged reasonably well. No use has been made of Padé approximants.

As expected, there is one (double) root $\beta = 0$, for, from equations (A 7) and (A 11) of the Appendix, we see that the elements of the first column of $\boldsymbol{A}_{22}$ are all zeros. Hence by (A 1) and (A 2) there is a solution in which $\beta = 0$, $a_0 \neq 0$ and all the other coefficients vanish. This corresponds to a purely horizontal shift of the surface profile through a distance a_0, without change of form.

Table 1 shows further that β has just one positive value, corresponding to an exponential rate of growth. All the remaining eigenvalues β are pure imaginary, corresponding to oscillatory normal modes.

The most interesting mode is clearly the exponentially growing mode. Table 1 shows that by $N = 50$ the corresponding value of β has converged effectively to

$$\beta = 0.0544\ldots. \tag{6.1}$$

The form of this mode is shown in figures 3 and 4, at successive times t, illustrating the exponential growth. The stability consists of a forward displacement of the fluid, confined mainly to the wave crest. The displacement begins rather abruptly at the 'toe' of the instability, which is located on the forward face of the unperturbed wave. The location of the toe can be defined as the point of maximum upwards curvature of the perturbation profile. This occurs at a horizontal distance $y \doteq -2.3$ from the centreline.

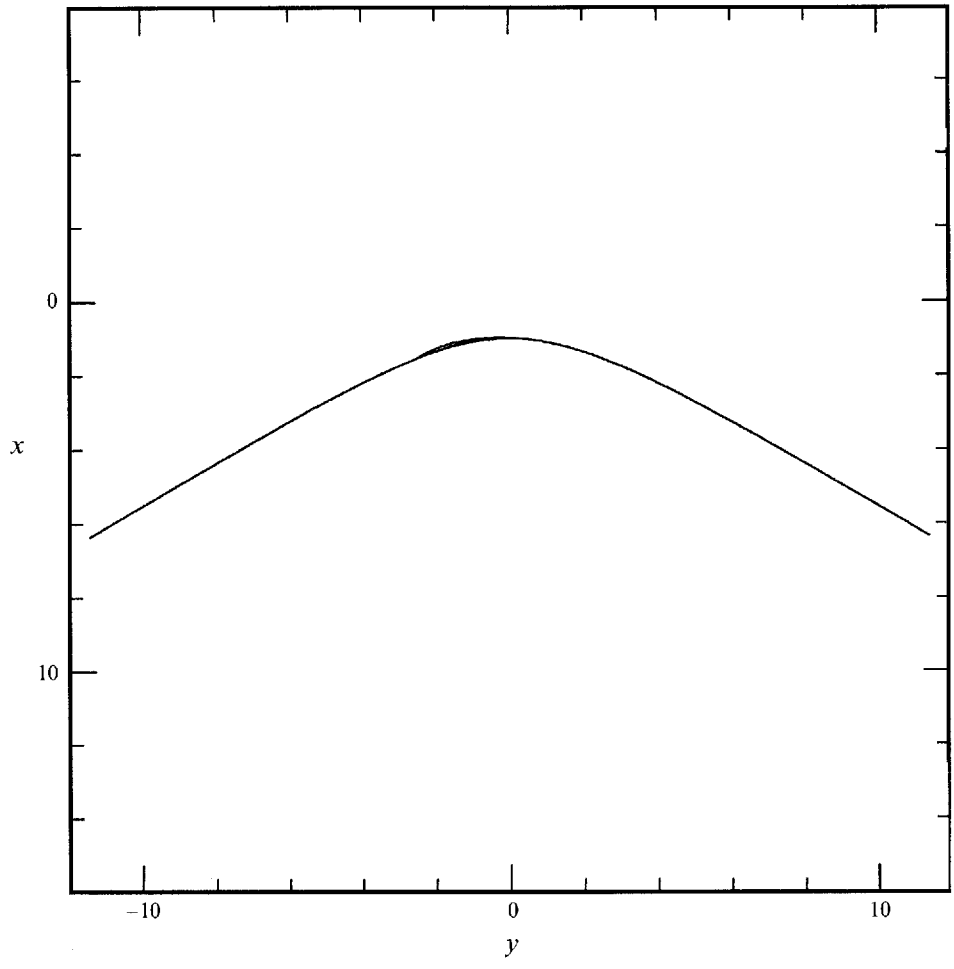

FIGURE 3. Profile of the unstable mode $\beta = 0.05442$ at times $t = 0$, 10, and 20. The amplitude α at $t = 0$ is 0.01.

N	$\pm\beta$	$\pm\sigma_1$	$\pm\sigma_2$	$\pm\sigma_3$	$\pm\sigma_4$	$\pm\sigma_5$
30	0.05452	0.00000	0.08000	0.26393	0.61308	0.80706
32	0.05447	0.00000	0.08026	0.26380	0.61313	0.80701
34	0.05444	0.00000	0.08045	0.26372	0.61316	0.80698
36	0.05443	0.00000	0.08058	0.26367	0.61318	0.80697
38	0.05442	0.00000	0.08068	0.26364	0.61320	0.80696
40	0.05442	0.00000	0.08075	0.26362	0.61321	0.80695
42	0.05442	0.00000	0.08081	0.26361	0.61322	0.80695
44	0.05442	0.00000	0.08086	0.26360	0.61322	0.80694
46	0.05443	0.00000	0.08090	0.26359	0.61322	0.80694
48	0.05443	0.00000	0.08093	0.26359	0.61323	0.80694
50	0.05444	0.00000	0.08097	0.26359	0.61323	0.80694

TABLE 1. Calculated growth rates β and eigenfrequencies $\sigma_m = \mathrm{i}\beta_m$ for the lowest normal modes, when $N = 30(2)50$.

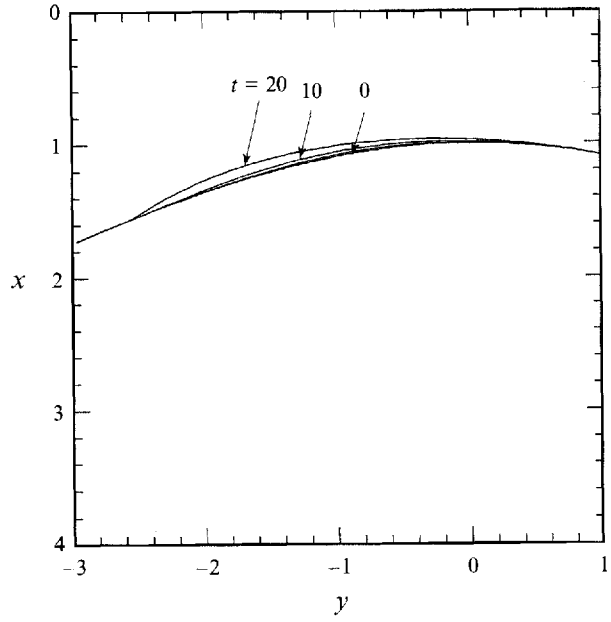

FIGURE 4. Close-up of the profile in figure 3.

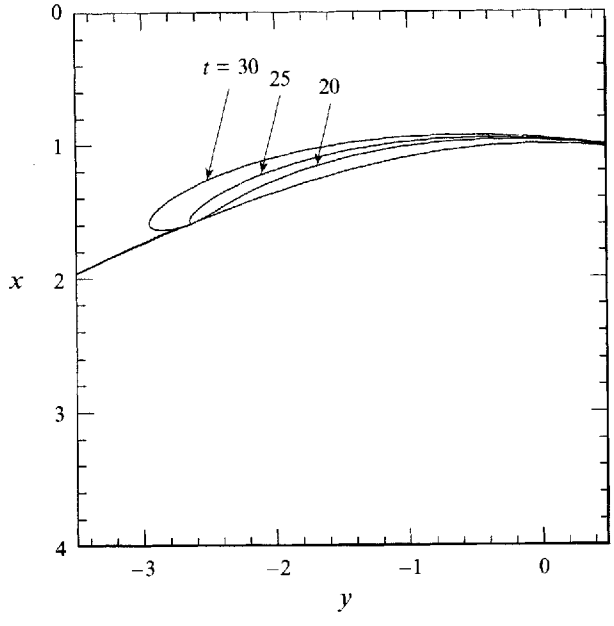

FIGURE 5. As in figure 3, but at times $t = 20$, 25 and 30, indicating qualitatively the later development of the instability.

The tangent to the unperturbed surface at this point makes an angle of 21° with the horizontal.

It will be realized that the present analysis is valid for a small perturbation only. If the amplitude of the perturbation were increased, the theoretical profile would develop as in figure 5, so that the crest would overturn. But one criterion for the validity of the perturbation expansion is that the corresponding perturbation in the surface slope

should not be too large. Thus figure 5 is at best a qualitative indication of the later development of the flow. A more realistic form is likely to be as in the rough analytic model given by Longuet-Higgins (1981, figures 7 and 12), in which the forward face of the wave has a finite concave curvature. A strong forwards jet can then erupt from the tip of the wave (see for example Longuet-Higgins & Cokelet 1976, 1978). However, these later, nonlinear shapes of the flow must be treated by different analytic models, or else by numerical time stepping.

By reversing the sign of the eigenvector $\boldsymbol{x}$ in (5.24) we obtain a perturbation which has a toe on the *rear* face of the wave. Such instabilities are less often observed. This may be due to the fact that any small disturbances on the forward face of the wave are accentuated by orbital straining, whereas on the rear face they are diminished. The sign of the instability is that corresponding to an excitation of the forward face, rather than the rear face.

The remaining eigenvalues in table 1 correspond to purely harmonic oscillations of the flow, without exponential growth. An example is shown in figure 6. This corresponds to a bound progressive wave superposed on the unperturbed flow, which is being swept backwards over the wave crest. Its relative phase speed is much smaller than the (backwards) velocity of the unperturbed flow, in the chosen frame of reference.

Returning to the unstable of figure 3, we may convert the rate of instability to more practical units as follows.

The radius of curvature at the crest of the unperturbed profile is

$$R = 5.15 \tag{6.2}$$

in the present units (see LHF1, §9). From dimensional considerations, since the only physical constant involved is the acceleration due to gravity g, the rate of growth β must be of the form

$$\beta = C(g/R)^{\frac{1}{2}}, \tag{6.3}$$

where C is an absolute constant. In the present units $g = 1$, hence

$$C = 0.0544 \times (5.15)^{\frac{1}{2}} = 0.123. \tag{6.4}$$

It can also be shown that the e-folding time of the instability is about two and a half times the time taken for a particle near the crest to traverse a diameter of the circle of curvature.

In a progressive gravity wave of length 2π, the ratio of the lengthscales is equal to ϵ^2 (see LHF1, equation (2.4)) where ϵ is the parameter defined by equation (2.5) above. The ratio of the timescales is therefore ϵ^1, by Froude scaling. For such a gravity wave the ratio of β to the radian frequency σ of a wave of small amplitude is

$$\beta/\sigma = 0.0544\epsilon^{-1}. \tag{6.5}$$

Lastly, to relate ϵ to the steepness parameter ak of the gravity wave, we have, from equation (5.4) of LHF1,

$$ak = 0.443 - 0.50\epsilon^2 + O(\epsilon^3), \tag{6.6}$$

so that

$$\epsilon^2 \doteq 2\Delta ak \tag{6.7}$$

where Δak denotes the difference between ak and its limiting value 0.4432. From (6.6) we then have

$$\beta/\sigma = 0.0385(\Delta ak)^{-\frac{1}{2}}. \tag{6.8}$$

This shows that for very steep waves (if they are attainable) the rate of growth, on a fixed timescale, goes to infinity like $(\Delta ak)^{-\frac{1}{2}}$.

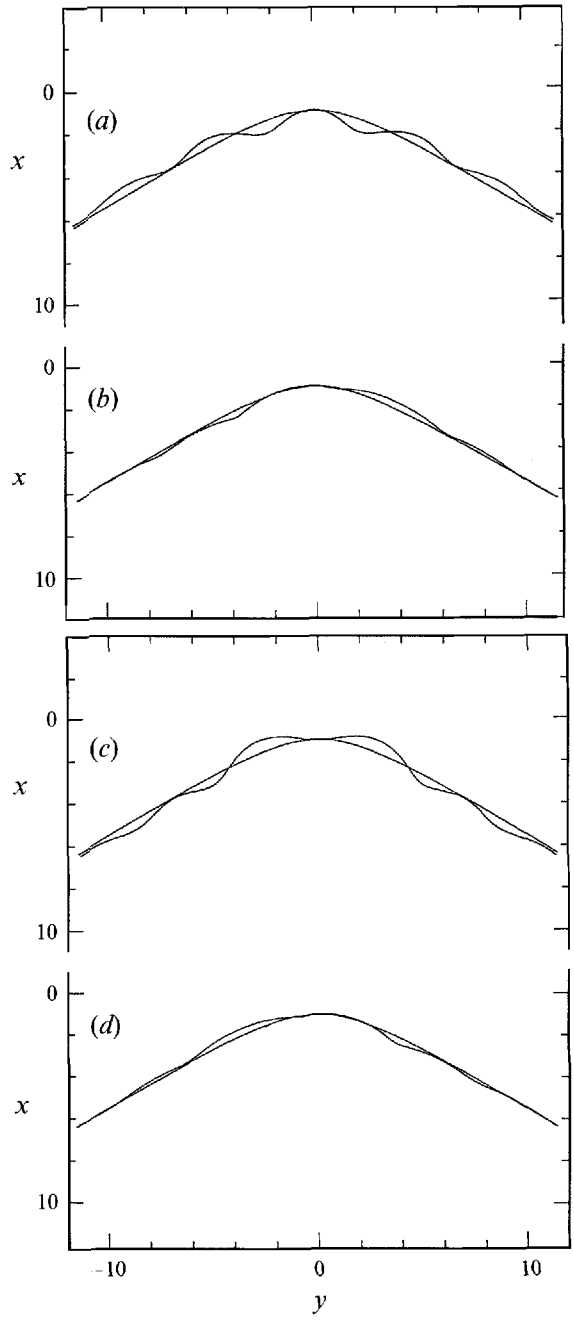

FIGURE 6. Profiles of the neutrally stable mode $\sigma = 0.263\,59$ at four different phases. (*a*) $\sigma t = 0$, (*b*) $\sigma t = \frac{1}{2}\pi$, (*c*) $\sigma t = \pi$, (*d*) $\sigma t = 2\pi$.

7. Discussion

The existence of an inherent instability in the crest of a steep gravity wave has important implications for the way in which two-dimensional gravity waves actually break. From our results it seems extremely unlikely that a steep wave will attain the Stokes limiting form; in practice it must topple over before that steepness is attained.

In previous theoretical work on periodic, irrotational waves (Tanaka 1983; Longuet-

Higgins 1986) it was found that the lowest superharmonic perturbation became unstable at around $ak = 0.4292$, corresponding to the lowest energy maximum. The instability analysed in the present paper is very probably a limiting form of this same instability. To trace the connection requires that we consider the stability of a wave crest modified by an 'outer flow' corresponding to the rest of the wave, as was described in Longuet-Higgins & Fox (1978). We shall carry out this analysis in future work. The present paper has established that there is an instability which is essentially a local property of an isolated wave crest, and hence may occur in other types of wave, for example waves in finite depth, or in irregular seas.

On a small scale, where surface tension forces become significant, there arises the interesting possibility that the true source for the parasitic capillary waves found on the forward face of a short gravity wave is not the sharp negative curvature at the gravity wave crest itself, as has been previously suggested, but rather the sharp (positive) curvature occurring at the 'toe' of the crest instability. This conclusion appears to be consistent with many careful observations of parasitic capillaries. A full analysis will involve the incorporation of surface tension into the boundary conditions.

The present paper is based in part on Chapters 5 to 7 of R.P.C.'s PhD dissertation (Cleaver 1981); the numerical calculations have been revised and extended by M.S.L.-H. who is indebted to Jon Wright for advice on eigenvector subroutines. The work has been supported by the Office of Naval Research under Contract N00014-91-J-1582.

Appendix. Calculation of the eigenvalues

It will be seen that the order of equation (5.25) can be reduced by splitting the vector $\boldsymbol{x}$ into two halves. Thus if we write

$$\boldsymbol{u} = (a_0, a_1, \ldots, a_N; d_1, d_2, \ldots, d_N), \quad \boldsymbol{v} = (b_0, b_1, \ldots, b_N; c_1, c_2, \ldots, c_N) \tag{A 1}$$

equation (5.25) becomes

$$\beta \boldsymbol{A}_{11}\boldsymbol{u} = \boldsymbol{A}_{12}\boldsymbol{v}, \quad \beta \boldsymbol{A}_{21}\boldsymbol{v} = \boldsymbol{A}_{22}\boldsymbol{u}, \tag{A 2}$$

where $\boldsymbol{A}_{11}$ denotes the matrix derived from the terms proportional to $\cos n\tau$ in the first of the two equations (5.22), together with the terms proportional to $\sin n\tau$ in the second equation, and so on.

Thus we can write

$$\boldsymbol{A}_{11}: \begin{cases} \operatorname{Im}[P(w)\,C(w)], & \frac{1}{2}, \cos n\tau \\ \operatorname{Re}[P(w)\,C(w)] - R(\tau)\,F(\tau), & \sin n\tau \end{cases}, \tag{A 3}$$

and similarly

$$\boldsymbol{A}_{21}: \begin{cases} \operatorname{Re}[Q(w)\,E(w) - R(w)\,C(w)] + S(\tau)\,F(\tau), & \frac{1}{2}, \cos n\tau \\ -2(1+\cos\tau)\,\mathrm{d}F/\mathrm{d}\tau, & \sin n\tau \end{cases}, \tag{A 4}$$

$$\boldsymbol{A}_{21}: \begin{cases} \operatorname{Re}[P(w)\,C(w)] - R(\tau)\,F(\tau), & \frac{1}{2}, \cos n\tau \\ \operatorname{Im}[P(w)\,C(w)] & \sin n\tau \end{cases}, \tag{A 5}$$

$$\boldsymbol{A}_{22}: \begin{cases} -2(1+\cos\tau)\,\mathrm{d}F/\mathrm{d}\tau & \frac{1}{2}, \cos n\tau \\ \operatorname{Re}[Q(w)\,E(w) - R(w)\,C(w)] + S(\tau)\,F(\tau), & \sin n\tau \end{cases}, \tag{A 6}$$

where n runs from 1 to N. In the case $n = 0$ it is convenient to take the constant in the Fourier series to be $\frac{1}{2}$ rather than 1. This multiplies the corresponding coefficients by 2.

In this way we find

$$\boldsymbol{A}_{11} = \begin{pmatrix} \boldsymbol{P}^{(+)} & \vdots & \boldsymbol{0} \\ \cdots & & \cdots \\ \boldsymbol{P}^{(-)} & \vdots & \boldsymbol{R}^{-} \end{pmatrix}, \qquad \boldsymbol{A}_{12} = \begin{pmatrix} \boldsymbol{Q}-\boldsymbol{R}^{(+)} & \vdots & \boldsymbol{S}^{(+)} \\ \cdots & & \cdots \\ \boldsymbol{0} & \vdots & \boldsymbol{J}' \end{pmatrix}, \tag{A 7}$$

$$\boldsymbol{A}_{21} = \begin{pmatrix} \boldsymbol{P}^{(+)} & \vdots & -\boldsymbol{R}^{(+)} \\ \cdots & & \cdots \\ -\boldsymbol{P}^{(-)} & \vdots & \boldsymbol{0} \end{pmatrix}, \quad \boldsymbol{A}_{22} = \begin{pmatrix} 0 & \vdots & -\boldsymbol{J} \\ \cdots & & \cdots \\ -\boldsymbol{Q}'-\boldsymbol{R}^{(-)} & \vdots & -\boldsymbol{S}^{(-)} \end{pmatrix}, \tag{A 8}$$

where in the case $N = 3$, for example,

$$\boldsymbol{P}^{(+)} = \begin{pmatrix} (P_0+P_0) & (P_{-1}+P_{-1}) & (P_{-2}+P_{-2}) & (P_{-3}+P_{-3}) \\ (P_{-1}+P_1) & (P_{-2}+P_0) & (P_{-3}+P_{-1}) & (P_{-4}+P_{-2}) \\ (P_{-2}+P_2) & (P_{-3}+P_1) & (P_{-4}+P_0) & (P_{-5}+P_{-1}) \\ (P_{-3}+P_3) & (P_{-4}+P_2) & (P_{-5}+P_1) & (P_{-6}+P_0) \end{pmatrix}, \tag{A 9}$$

$$\boldsymbol{P}^{(-)} = \begin{pmatrix} (P_{-1}-P_1) & (P_{-2}-P_0) & (P_{-3}-P_{-1}) & (P_{-4}-P_{-2}) \\ (P_{-2}-P_2) & (P_{-3}-P_1) & (P_{-4}-P_0) & (P_{-5}-P_{-1}) \\ (P_{-3}-P_3) & (P_{-4}-P_2) & (P_{-5}-P_1) & (P_{-6}-P_0) \end{pmatrix} \tag{A 10}$$

and

$$\boldsymbol{Q} = \begin{pmatrix} 0\cdot(Q_0+Q_1) & 2(Q_{-1}+Q_0) & 4(Q_{-2}+Q_{-1}) & 6(Q_{-3}+Q_{-2}) \\ 0\cdot(Q_1+Q_2) & 1\cdot(Q_0+Q_1) & 2(Q_{-1}+Q_0) & 3(Q_{-2}+Q_{-1}) \\ 0\cdot(Q_2+Q_3) & 1\cdot(Q_1+Q_2) & 2(Q_0+Q_1) & 3(Q_{-1}+Q_0) \\ 0\cdot(Q_3+Q_4) & 1\cdot(Q_2+Q_3) & 2(Q_1+Q_2) & 3(Q_0+Q_1) \end{pmatrix}. \tag{A 11}$$

$\boldsymbol{Q}'$ is the same as $\boldsymbol{Q}$ but without the first row. Also $\boldsymbol{R}^{(+)}$ is similar to $\boldsymbol{P}^{(+)}$ but without the first column while

$$\boldsymbol{R}^{(-)} = \begin{pmatrix} (R_{-1}-R_1) & (R_{-2}-R_0) & (R_{-3}-R_{-1}) & (R_{-4}-R_{-2}) \\ (R_{-2}-R_2) & (R_{-3}-R_1) & (R_{-4}-R_0) & (R_{-5}-R_{-1}) \\ (R_{-3}-R_3) & (R_{-4}-R_2) & (R_{-5}-R_1) & (R_{-6}-R_0) \end{pmatrix}. \tag{A 12}$$

$\boldsymbol{R}^{-}$ denotes $\boldsymbol{R}^{(-)}$ without the first column. Then $\boldsymbol{S}^{(+)}$ is similar to $\boldsymbol{R}^{(+)}$, while

$$\boldsymbol{S}^{(-)} = \begin{pmatrix} (S_{-2}-S_0) & (S_{-3}-S_{-1}) & (S_{-4}-S_{-2}) \\ (S_{-3}-S_1) & (S_{-4}-S_0) & (S_{-5}-S_{-1}) \\ (S_{-4}-S_2) & (S_{-5}-S_1) & (S_{-6}-S_0) \end{pmatrix}. \tag{A 13}$$

Lastly,

$$\boldsymbol{J} = \begin{pmatrix} 2 & 0 & 0 \\ 2 & 2 & 0 \\ 1 & 4 & 3 \\ 0 & 2 & 6 \end{pmatrix}, \tag{A 14}$$

while $\boldsymbol{J}'$ is the same as $\boldsymbol{J}$ but without the first row. Note that the first rows of $\boldsymbol{J}$ and $\boldsymbol{Q}$ are double the values corresponding to the pattern in the matrices as a whole.

From (A 2) one obtains immediately

$$\beta \boldsymbol{u} = \boldsymbol{B}_1 \boldsymbol{v}, \quad \beta \boldsymbol{v} = \boldsymbol{B}_2 \boldsymbol{u}, \tag{A 15}$$

where $\boldsymbol{B}_1 = \boldsymbol{A}_{11}^{-1}\boldsymbol{A}_{12}$ and $\boldsymbol{B}_2 = \boldsymbol{A}_{21}^{-1}\boldsymbol{A}_{22}$. Whence

$$\beta^2 \boldsymbol{u} = \boldsymbol{B}_1 \boldsymbol{B}_2 \boldsymbol{u}. \tag{A 16}$$

Therefore $\lambda = \beta^2$ is a root of the eigenvalue equation

$$\det(\boldsymbol{B}_1 \boldsymbol{B}_2 - \lambda \boldsymbol{I}) = 0. \tag{A 17}$$

For a given order N of truncation, the matrix $\boldsymbol{B}_1 \boldsymbol{B}_2$ has $(2N+1)$ rows and columns, half the number corresponding to the matrices in (5.23). We can therefore expect improved accuracy and speed of solution, at a given value of N.

REFERENCES

BANNER, M. L. & PEREGRINE, D. H. 1993 Wave breaking in deep water. *Ann. Rev. Fluid Mech.* **25**, 373–397.

BONMARIN, P. 1989 Geometric properties of deep-water breaking waves. *J. Fluid Mech.* **209**, 405–433.

CLEAVER, R. P. 1981 Instabilities of surface gravity waves. PhD thesis, University of Cambridge, UK, 224 pp.

HOLTHUIJSEN, L. H. & HERBERS, T. H. C. 1986 Statistics of breaking waves observed as white-caps in the open sea. *J. Phys. Oceanogr.* **16**, 290–297.

KJELDSEN, S. P. & MYRHAUG, D. 1980 Wave–wave interactions current-wave interactions and resulting extreme waves and breaking waves. *Proc. 17th Intl Conf. Coastal Engng*, pp. 2277–2303. ASCE.

LONGUET-HIGGINS, M. S. 1978*a* Some new relations between Stokes's coefficients in the theory of gravity waves. *J. Inst. Maths Applics.* **22**, 261–273.

LONGUET-HIGGINS, M. S. 1978*b* The instabilities of gravity waves of finite amplitude in deep water. I. Superharmonics. *Proc. R. Soc. Lond.* A **360**, 471–488.

LONGUET-HIGGINS, M. S. 1981 On the overturning of gravity waves. *Proc. R. Soc. Lond.* A **376**, 377–400.

LONGUET-HIGGINS, M. S. 1986 Bifurcation and instability in gravity waves. *Proc. R. Soc. Lond.* A **403**, 167–187.

LONGUET-HIGGINS, M. S. 1988 Mechanisms of wave breaking in deep water. In *Sea Surface Sound* (ed. B. R. Kerman), pp. 1–30. Kluwer. 639 pp.

LONGUET-HIGGINS, M. S., CLEAVER, R. P. & FOX, M. J. H. 1994 Crest instabilities of gravity waves. Part 2. Matching and asymptotic expansion. *J. Fluid Mech.* **259**, 333–344.

LONGUET-HIGGINS, M. S. & COKELET, E. D. 1976 The deformation of steep gravity waves. I. A numerical method of computation. *Proc. R. Soc. Lond.* A **350**, 1–26.

LONGUET-HIGGINS, M. S. & COKELET, E. D. 1978 The deformation of steep gravity waves on water. II. Growth of normal-mode instabilities. *Proc. R. Soc. Lond.* A **364**, 1–28.

LONGUET-HIGGINS, M. S. & FOX, M. J. H. 1977 Theory of the almost-highest wave: the inner solution. *J. Fluid Mech.* **80**, 721–741 (referred to herein as LHF1).

LONGUET-HIGGINS, M. S. & FOX, M. J. H. 1978 Theory of the almost-highest wave. Part 2. Matching and analytic extension. *J. Fluid Mech.* **85**, 769–786.

MICHELL, J. H. 1893 The highest waves in water. *Phil. Mag.* **36**, 430–437.

TANAKA M. 1983 The stability of steep gravity waves. *J. Phys. Soc. Japan* **52**, 3047–3055.

TULIN, M. P. & LI, J. J. 1991 A mechanism for wave deformation and breaking intermediated by resonant side-bands. *Proc. IUTAM Symp. on Breaking Waves, Sydney, Australia July 1991* (ed. M. L. Banner & R. H. J. Grimshaw), pp. 21–37. Springer.